NUREG/CR-0521
LA-7571-MS

Informal Report

C.3

Analysis of Nuclear Facilities for

Tornado-Induced Flow and Reentrainment

University of California

LOS ALAMOS SCIENTIFIC LABORATORY

Post Office Box 1663   Los Alamos. New Mexico 87545

Affirmative Action/Equal Opportunity Employer

Analysis of Nuclear Facilities for

Tornado-Induced Flow and Reentrainment

R. W. Andrae
R. A. Martin
W. S. Gregory

ANALYSIS OF NUCLEAR FACILITIES

FOR

TORNADO-INDUCED FLOW AND REENTRAINMENT

by

R. W. Andrae, R. A. Martin, and W. S. Gregory

ABSTRACT

This report describes an analytical procedure that may be used to calculate tornado-induced flow and material reentrainment within nuclear fuel cycle facilities. The procedure involves the following four steps.
(1) A computer code models the overall ventilation pathways and predicts tornado-induced flows and pressures.
(2) A second computer code models individual rooms or cells and predicts velocities within the room induced by the flows from step (1).
(3) These velocities are then used to predict reentrainment and suspension of particulate material.
(4) The possibility of release is predicted from the flow patterns calculated in (1).
For illustrative purposes only, the head-end ventilation system of the Nuclear Fuel Services, West Valley, New York, plant was analyzed using the proposed procedure.

I. INTRODUCTION

The transient depressurization associated with a tornado contacting the air supply and exhaust points of nuclear facilities can cause significantly higher-than-normal flows and pressure differences within the facilities.[1] Consequently, under tornado conditions, relatively high air velocities can occur over interior surfaces of ducts, isolation cells, and gloveboxes where deposits of radioactive material may be present. These velocities, if sufficiently high, can in turn cause quantities of radioactive material to become

suspended and possibly transported through ventilation pathways and ultimately to air release points.

An analytical procedure that can predict the potential for release of hazardous material from a tornado-induced flow is essential to safety reviews of existing fuel cycle facilities and for preparing criteria for new plant licensing. The purpose of this report is to outline such a procedure, but it should be considered preliminary because the analytical tools used were not developed explicitly for the stated purpose and only a short period of time was available.

Two computer codes developed at the Los Alamos Scientific Laboratory were used. These codes are described below and in greater detail elsewhere.[2-4] A one-dimensional code, TVENT,[2,3] was used to calculate flow and pressure histories within the facility. The output from this code was then used for input as boundary conditions to another computer code, SOLA-ICE,[4] which calculates detailed two-dimensional, transient velocities in areas where deposited radioactive material is likely. Finally, these velocities were used together with assumptions of particulate and surface characteristics to calculate reentrained material quantities. An assessment of material release at the plant's atmospheric boundaries can then be made by considering system flow magnitudes and direction (from TVENT results).

To illustrate the procedure, we analyzed the head-end ventilation system of the Nuclear Fuel Services (NFS) fuel reprocessing plant near West Valley, New York. Although NFS operations were terminated in 1972, radioactive material remains in the main process cells. We have investigated the flow conditions throughout the entire NFS head-end ventilation system for one tornado condition, but we have chosen to illustrate the proposed procedure for the General Process Cell (GPC). Thus, detailed velocities and possible reentrainment of an assumed particulate from the GPC floor were investigated. However, we did not address the more general question of overall facility safety under all possible tornado conditions.

II. ANALYTICAL PROCEDURE

To determine if particulate material release would be possible under tornado conditions, assuming the ventilation system remains intact, we must answer five questions.

2

(1) What are the magnitude and direction of the system air flows?

(2) What are the detailed local air velocities near contaminated surfaces?

(3) Will reentrainment occur as a result of these velocities?

(4) If reentrainment does occur, how much material becomes suspended?

(5) How much, if any, of this suspended material could reach the system boundaries through the ductwork or other routes?

The flow chart shown in Fig. 1 depicts the analytical procedures used to answer these questions. The outputs of TVENT and SOLA-ICE answer questions (1) and (2), respectively. For a given room, the output of TVENT is converted into air velocities that become the boundary conditions for SOLA-ICE. Although SOLA-ICE calculates velocity distributions throughout the room, only those velocities adjacent to the surface under consideration were used in the reentrainment studies.

The answers to questions (3) and (4) do not involve the use of computer codes. As shown in Fig. 1, a velocity at the edge of the boundary layer obtained from SOLA-ICE is used to calculate the friction velocity u_*. This velocity is compared to a threshold friction velocity u_{*t}, obtained from empirical data to determine if reentrainment is possible. If reentrainment is possible ($u_* > u_{*t}$), then semi-empirical equations are used to calculate material quantities suspended.

Finally, consideration of suspended material release [question (5)] requires consideration of flow into and out of the GPC during the reentrainment period. Thus, additional examination of TVENT flow data is required to determine if the suspended material can indeed escape to the environment.

All of the steps outlined above are discussed in greater detail in the sections that follow. Assumptions and qualifications are also presented at each step in the procedure.

III. TVENT ANALYSIS

A. Modeling

The modeling parameters and the steady-state conditions were provided by the Oak Ridge National Laboratory (ORNL)[5] and are given in Fig. 2. The TVENT model constructed from these data is shown in Fig. 3, which simulates the portion of the NFS facility that involves the Process Building. The building houses the main process cells that have their own ventilation system
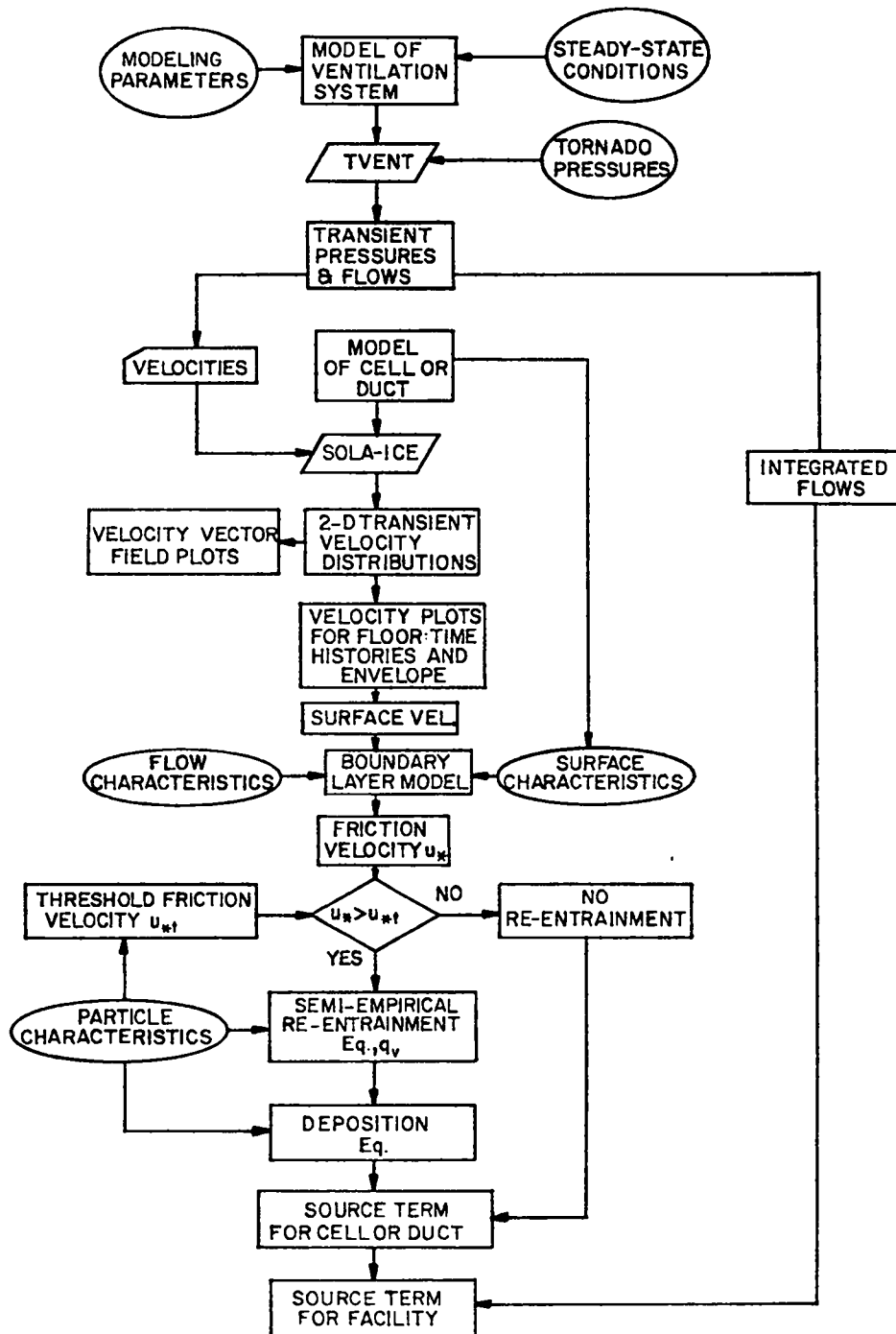
Fig. 1.
Analytical procedure flow chart.

METRIC CONVERSION FACTORS

1 cfm = 4.719 x 10^{-4} m^3/s
1 psi = 6.894 kPa
1 in.w.g. = .249 kPa
1 ft^3 = .0283 m^3
1 ft = 0.3048 m
1 mph = 0/447 m/s

Head-End Ventilation
System At NFS

0.0. 7 Intake
(6)

2000

8535

0.0
1
Intake (1)

-0.05
2
Corridor
(25000 CF)

(2)

-0.9
3
C.P.C
(87980 CF)

(3)

9 Decon. room (0.15)
(7524 CF)

(18) ΔP=5.35

1900

(19)

18

(20) Demister ΔP=0.3

19

(9)

ΔP   ΔP   ΔP   ΔP
0.5 Dirty 2.0   8.5   1.3
0.1 Clean 0.2   1.3   1.3

10300

-1.01

G.P.C
(9780 CF) 8

(8)

-14.5

7105
(15)

0.4   0.0
Exh.
17

(17)
Stack

10
(21)

20
(10)
Prefilter

11
(11)
Roughing

12
(12)
HEPA

14100
13
(13)
HEPA

14
(14)

15

16

-19.6
(16)
7105

(15500 CF)
P.M.C
-1.0

1727

0.0
4
Intake (4)

-0.1
5
Corridor
(15000 CF)

(5)

6

(7)

t(s) 0.0   3.25   7.25   10.5

0.0

P
(in H_2O)

-72.0

Tornado Transient
2.6 psi
0.8 psi/s
265 ft rad
55 mph

Head, in W.G.

35
30
25 22.6 Operating point
23 20 20.0
15
12.0
10
5

-2 0 2 4 6 8 10 12 14
Flow, (cfm x 10^{-3})
Blower Curve

Fig. 2.
Input data for head-end ventilation system.

5

NUCLEAR FUEL SERVICES (NFS)

Head End Ventilation System

↓Outside air

Outside Air

8585 CFM (4.05 m³/s)

Corridor 25,000 CF (708 m³) −0.05 in W.G (−0.012 kPa)

Filter

CPC 87,980 CF (2.491 m³) −0.90 in W.G. (−0.12 kPa)

Hatch

Decon. Room 7524 CF (213 m³) −0.15 in W.G. (−0.037 kPa)

1900 CFM (0.897 m³/s)

1700 CFM (0.802 m³/s)

Louvers ΔP = 2.0 in W.G (0.50 kPa)

Demister ΔP = 0.3 (0.07 kPa)

Roughing Filter

HEPA Filters

Prefilter

HEPA Filters

Louver

7100 CFM (3.35 m³/s)

−19.6 in W.G

04 in W.G.
To Stack

7100 CFM (3.35 m³/s)

GPC 9,780 CF (277 m³) −1.01 in W.G (−0.25 kPa)

−6.50 in W.G. (−1.62 kPa)

Roughing Filter

Louver

Prefilter

HEPA Filters

HEPA Filters

Outside Air

1715 CFM (0.809 m³/s)

Hatch

Corridor 15,000 CF (425 m³) −0.1 in W.G. (−0.025 kPa)

Filter

PMC 15,500 CF (439 m³) −1.0 in W.G. (−0.25 kPa)

Filter Pressure Drop Schedule

Filter	Dirty	Clean
Prefilter	0.15 in W.G (0.12 kPa)	0.1 (0.025)
Roughing Filter	2.0 (0.5)	0.2 (0.005)
1st bank HEPA's	8.5 (2.1)	1.3 (0.32)
2nd bank HEPA's	1.3 (0.32)	1.3 (0.32)

Blower Performance Curve
Manufacturer – Buffalo Forge
Type – 5 RPNW Size –35

Operating point 20.0
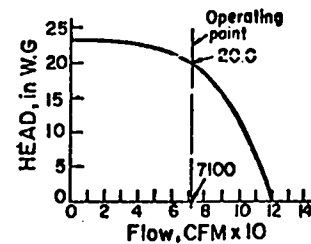
HEAD, in W.G

7100

Flow, CFM x 10

Fig. 3.
TVENT model of head-end ventilation system.

known as the head-end ventilation system. Certain simplifying assumptions have been made in those areas lacking substantiating data. A brief description of this part of the facility and mention of some of these assumptions follows.

The main process cells are (1) the Process Mechanical Cell (PMC) in which the fuel elements to be processed were cut into small pieces; (2) the GPC where the pieces were stored until a batch was ready for processing; and, (3) the Chemical Process Cell (CPC) in which the chemical dissolving took place. These cells are connected by hatchways. The covers for the hatchways are assumed to have been removed, and these passages form the only ventilation pathways. Both the PMC and the CPC are ventilated by outside air supplies. We assumed that these air supplies are exposed to the full effects of the tornado through loss of external building walls. The walls are actually constructed of reinforced concrete block. In addition, the filter between the cell and corridor, and the damper between the corridor and the intake are represented by lumped components to simulate the system resistance of these components. The resistances of the filters in the plenums upstream of the blowers are based on completely dirty conditions. The characteristics of the blowers are based on overcoming expected resistances for dirty filters.

ORNL also provided the tornado pressure transient shown in Fig. 2. The tornado had the following properties.

Maximum wind speed	145 m/s
Rotational speed	121 m/s
Translational speed	24.6 m/s
Radius of maximum rotational wind	80.8 m
Total pressure drop	17.9 kPa
Rate of pressure drop	5.5 kPa/s .

In the example problem used, the tornado is applied to all the supply points in the head-end system, at nodal points 1, 4, and 7. A 10-s period held at ambient pressure precedes the tornado to establish steady-state velocities in the cells. An echo of the input data is shown in Fig. A-1 in Appendix A.

B. Results

The possibility of air flowing from the GPC and being released at a supply point because of flow reversal is shown by plotting the flows in the paths

connecting the GPC and an outside air supply port on the same graph, Figs. A-2, A-3, and A-4. Release is possible only if the period of flow from the GPC coincides with a flow reversal at the supply ports, nodes 1, 4, or 7. This aspect of the problem is discussed in Sec. VI. Two other important output parameters are the flow velocities in the GPC hatches and duct and the amount of air going through these paths over a certain time. Both of these parameters are printed for each calculation time step. The velocities are based on the assumption of uniform flow. A sample of this listing is shown in Fig. A-5. The volume of air flowing during a specified time can be obtained by finding the difference between the integrated flows occurring at the beginning and end times for this period. This information is also needed in the branches connecting to the air supply points when the amount of air leaving the facility must be known.

IV. SOLA-ICE ANALYSIS

A. Modeling

The GPC has been selected for demonstrating the use of SOLA-ICE to obtain velocity distributions. Because of the two-dimensional aspects of the present code, modeling requires proper visualization and good judgment to simulate the effects occurring in a three-dimensional room. The model of the GPC used (Fig. 4) is essentially a vertical slice through the cell as indicated by the cross section shown in the isometric view. Two significant compromises were necessary in modeling. First, the exhaust duct shown dotted in the isometric view has been rotated 90° and translated so that all the flow paths are in the same plane. The other compromise concerns the magnitude of the boundary velocities for the duct and hatches. Actually, an airstream flowing from a constricted path into a larger volume expands, thereby reducing the velocity. This cannot be shown in a two-dimensional representation. This is a valid argument for reducing the boundary velocities by some factor to include this effect in calculating the floor velocities. Because a factor of 1 was used in this report, the air velocities near the floor are larger than they should be. The values of the velocity used are given in each printout of the calculated air velocities near the floor. All the functions generated in TVENT are shown even though they may not be used. These functions are numbered in the order they were punched in TVENT and do not retain their branch identification.
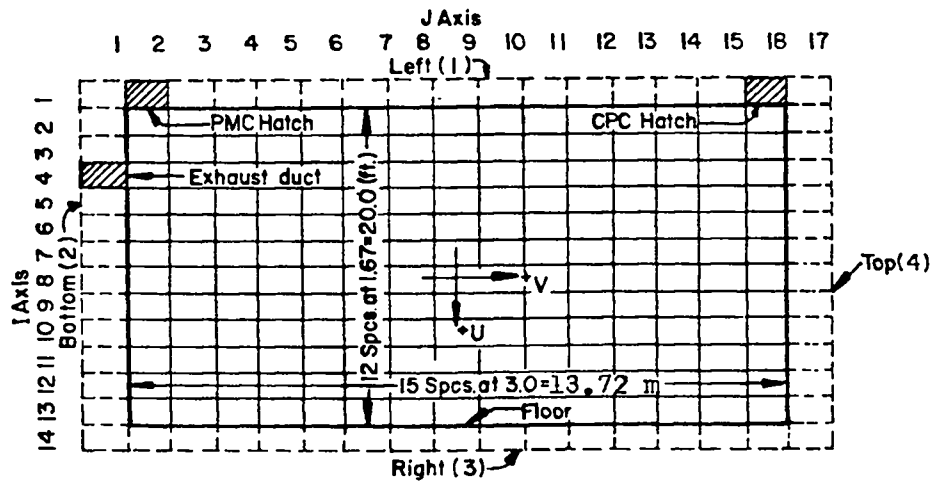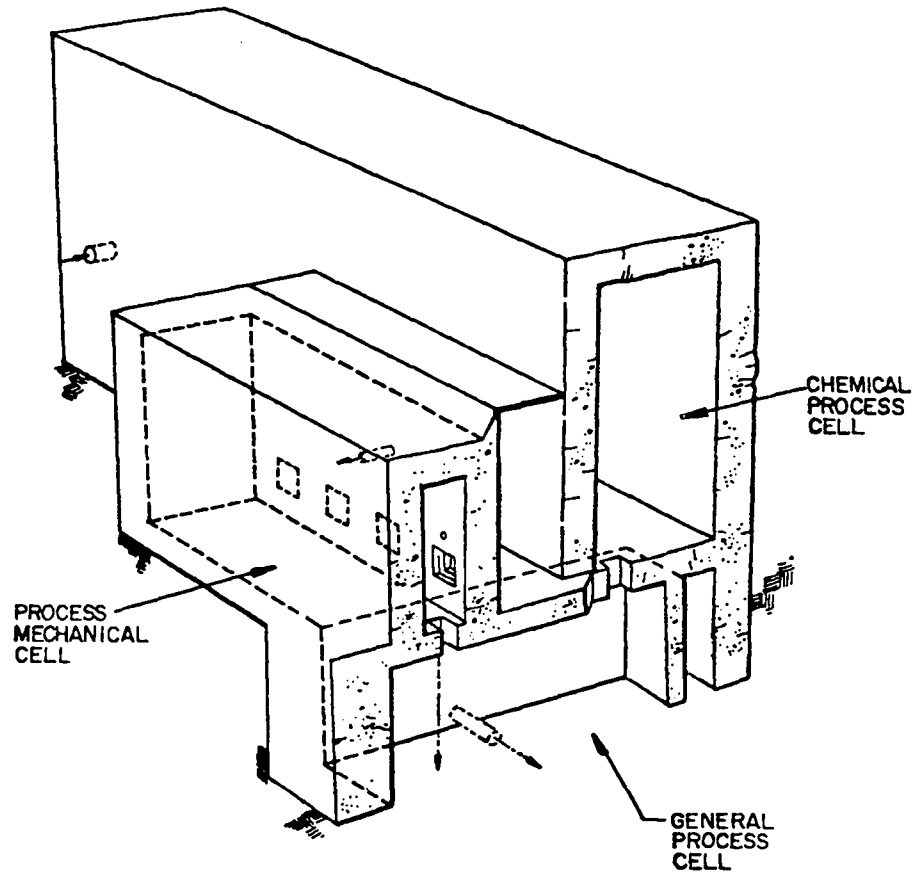
8

Fig. 4.
Location and details of SOLA-ICE plane through the GPC.

The input data other than the boundary velocities are presented in Fig. B-1 in Appendix B. A complete explanation of the required input and its formats is presented in Ref. 1 as modified by Appendix D of this report.

B. Results

SOLA-ICE results are displayed in three ways: (1) velocity vector plots (Fig. B-2); (2) velocity plots along the floor (Figs. B-3 to B-6); and (3) printouts of air velocities near the floor (Fig. B-7). The vector plots show the GPC cell flow patterns at a given time. There are two types of velocity plots along the floor: one is a composite of all the velocity vs time curves that describes envelopes for the air velocities near the floor, as shown in Fig. B-3, and the other shows velocity histories at a particular location along the floor, as shown in Figs. B-4 to B-6. (All the velocities near the floor are for the centers of elements I = 13 and J = 2 to 18 shown in the model.)

V. SOURCE TERM ESTIMATES

A. General

In this section we describe the problem of estimating the quantity of particulate material that can be reentrained from the GPC floor during tornado-induced transient flow conditions. (Reentrainment elsewhere in the plant including ductwork was not considered.) Here we propose a new analytical approach for calculating reentrainment that takes advantage of the detailed flow information available from TVENT and SOLA-ICE. After introducing the technique, we state our assumptions and qualifications and then present GPC source term estimate example calculations and results. We emphasize that these calculations have been performed for illustrative purposes only. The particulate size distribution and density used in these calculations were strictly hypothetical.

To arrive at an estimate of the quantity of material reentrained, we must answer the following questions. (1) When do particles begin to move? (2) What determines whether particles go into suspension? (3) How much material is suspended? and, (4) Does the material stay suspended or does it redeposit? A valid answer to (1) implies that one has taken into account particle, surface, and flow characteristics. Some account must also be made for the forces acting, namely, aerodynamic, interparticle (cohesion), and surface to particle (adhesion).

The resuspension factor K has been used extensively in the past to estimate reentrainment. Unfortunately, this concept bypasses questions (1) and (2) to answer (3) directly. By definition,

$$K = \frac{\text{air concentration } (g/m^3)}{\text{surface concentration } (g/m^2)} , \ 1/m .$$

Healy[6] reviewed measurements and applications of this simplistic concept and pointed out some of its limitations. Several points are of major concern to us. First, measured values of K range over 11 orders of magnitude. For benign conditions when K is most reliable, the uncertainty is at least two orders of magnitude. Also, K fails to account for particle, surface, or local flow characteristics. As a result, the resuspension factor would have to be measured for innumerable cases to encompass accident conditions. These problems render K essentially unworkable for our purposes.

The proposed new reentrainment calculational procedure has been discussed in detail elsewhere[7] and addresses each of the above four questions. This procedure is similar' to the approach taken by Travis,[8] who developed a computer model to predict reentrainment and redistribution of soil contaminants as a result of eolian effects. It was used here to estimate the number of grams of material that could be suspended over the floor of the GPC. Once airborne in the GPC, suspended material might enter the ventilation system during or after the transient, depending on flow magnitudes and directions. We will return to considerations of the likelihood of a release of entrained material later.

The flow chart shown in Fig. 1 includes our NFS reentrainment calculational procedure. We will summarize the steps briefly here. (The reader can find the necessary equations in Appendix C and additional details in Sec. V. D.) After TVENT, the SOLA-ICE code was run to provide required values of air flow velocities u near the GPC floor. These values and a boundary layer profile equation were used to calculate a surface friction velocity u_*. This value of u_* was compared to a threshold friction velocity u_{*t} for the assumed particulate material. This value of u_{*t} was estimated from the experimental data shown in Fig. 5. For this case we found $u_* > u_{*t}$ so some material could be set in motion. A semi-empirical reentrainment equation was used to estimate the flux of material that could become suspended q_v. Knowing q_v, the GPC
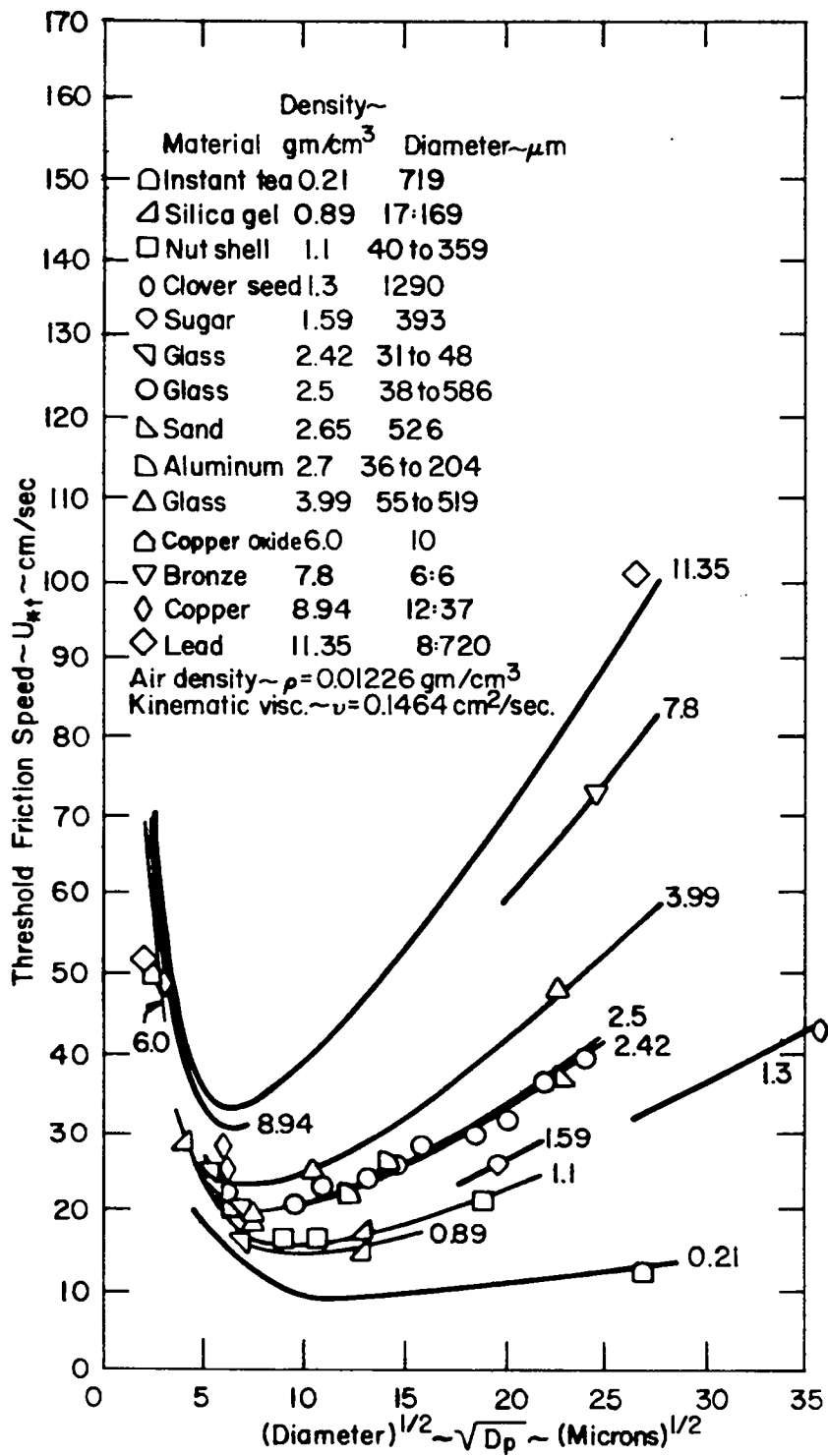
Fig. 5.
Threshold friction speed u_{*t} vs particle size.

floor area, and the time interval Δt over which u_* exceeds u_{*t}, we estimated a source term quantity of material M for the GPC in grams. Finally, a deposition velocity u_d was calculated that, together with the GPC volume, allowed an estimate of the mass deposition flux and time for depletion of the aerosol plume.

B. Assumptions

To compute the GPC source term, we need information about the particulate, the GPC floor, and air flow characteristics as well as a mapping of the surface loading (location and quantity). For an illustrative calculation, we have used flow information calculated by SOLA-ICE together with the following assumptions. The particulate is assumed to be spherical and have a diameter (D_p) less than 50 μm with a median diameter of 25 μm. Because all the particulates are smaller than 50 μm, we assume that all the material is suspendable. The average density ρ_p is assumed to be 3 g/cm^3. Note that this particulate is strictly hypothetical. We consider two surfaces: (1) a smooth surface like stainless steel or linoleum, and (2) a moderately rough surface with a roughness length of y_0 = 0.0104 cm (coarse sand). In both cases the floor is assumed to be flat without obstacles or protuberances. We further assume that the particulate loading is uniform over the entire floor and at least two particles deep. Also, we assume that standard atmospheric conditions prevail.

For the purpose of this reentrainment calculation, namely, to illustrate the technique, SOLA-ICE has produced more detailed flow information than we wish to use. That is, while velocities near the GPC floor have been calculated for 16 elements, the scope of this exercise will not permit a correlation of the SOLA-ICE-predicted velocity variation along the floor with local entrainment. Hence, for simplicity we make the assumption that the near-surface velocity time history illustrated in Fig. B-5 is representative of the entire floor. Figure B-3 shows that this is a conservative assumption. The boundary layer on the floor is assumed to be turbulent and 10 cm thick (so that u above 10 cm is constant). With these assumptions and knowing the total quantity of material present on the GPC floor, we can estimate the quantity of material reentrained subject to the following qualifications.

C. Qualifications

The question of how heavily a surface must be loaded before equations like Eqs. (C-2), (C-5), and (C-6) are applicable is debatable. For the realistic

13

types of loadings such as we expect to find in the GPC, the empirical constant in Eq. (C-6) may not be satisfactory because it was obtained for relatively thick powder beds. Furthermore, the empirical coefficients in Eq. (C-5) are suspect because they were obtained from experiments with soil particles.

The recent experimental and theoretical work underlying Eqs. (C-2) and (C-6) is believed to be the best available.[9-11] Thus, the basis for predicting u_{*t} using Eq. (C-2) is sound; however, the data base to which Eq. (C-2) was fit is sparse for small particles. In principle these uncertainties could be checked and reduced with appropriate experimentation.

D. Re-entrainment Calculational Procedure and Results of Example Calculations for the GPC

For the assumed particulate, we find u_{*t} = 28 cm/s (Fig. 5). Now entrainment can occur only if $u_* \geq u_{*t}$ = 28 cm/s. To relate this value of u to u at 10 cm above the floor, we apply Eqs. (C-3) and (C-4) for (1) a smooth surface, and (2) a rough surface with y = 0.0104 cm, respectively. The results are u_t = 6.55 m/s for case (1) and u_t = 4.8 m/s for case (2), where u_t is the free stream threshold velocity in each case. That is, if the free stream velocity u exceeds u_t = 4.8 m/s in case (2), for example, then we expect particulate reentrainment and suspension (since D_p < 50 μm). Referring to the SOLA-ICE output shown in Fig. B-5, we observe that u exceeds u_t in both cases for subintervals of 20 ≤ t ≤ 31 s. We have determined average values of u for each case using

$$u_{avg} = \frac{1}{t_2 - t_1} \int_{t_1}^{t_2} (|u| - u_t)dt ,$$

where $t_2 - t_1$ is the interval for which u exceeds u_t in each case. For case (1), t = $t_2 - t_1$ = 26.9 - 22.25 = 4.65 s, and for case (2), t = 30.5 - 21.35 = 9.15 s. Dropping "avg," the results are u = -7.56 m/s for case (1) and u = 6.61 m/s for case (2). Going back to Eqs. (C-3) and (C-4), the corresponding values of u_* are 31.8 cm/s for case (1) and 38.5 cm/s for case (2). Notice that for both cases u_* exceeds u_{*t} = 28 cm/s, so we expect particulate suspension for both cases. The time intervals used to calculate suspension are taken to be those associated with surface flow at the average values of u. These are Δt = 24.9 - 22.65 = 2.25 s for case (1), and Δt = 26.8 - 22.3 = 4.50 s for case (2).

14

We can use the latest values of u_* to calculate q_h and q_v from Eqs. (C-6) and (C-5), respectively. The results are $q_v = 2.77 \times 10^{-8}$ g/cm^2 s for case (1), and $q_v = 5.61 \times 10^{-5}$ g/(cm^2 s) for case (2). Finally, knowing the GPC floor area of $A = 4.70 \times 10^5$ cm^2 and Δt, we can calculate the total mass of suspended particulate using $M = q_v(A)(\Delta t)$. The results are $M = 2.93 \times 10^{-2}$ g for case (1) and $M = 119$ g for case (2). Note that in both cases we assumed that sufficient material was present on the floor to sustain the entrainment flow q_v over the entire Δt. Thus, these values of M are the maximum amounts of material that could be entrained. If less than M grams of material are present, it would all be entrained in less time than Δt.

Finally, using Eq. (C-8) we calculate a fall speed of $u_f = 5.74$ cm/s for the assumed particulate. For case (2) using $M = 119$ g, the GPC volume of 2.79×10^8 cm^3, and assuming the deposition velocity u_d is equal to u_f, we calculate a room concentration of $\Omega = 4.27 \times 10^{-7}$ g/cm^3, a deposition rate of 1.15 g/s, and a time for complete depletion of the aerosol cloud of 103 s. These calculations are summarized in Table I.

VI. DISCUSSION

The results of TVENT and SOLA-ICE supply data for the reentrainment calculation and are used to determine the possibility of particulate-laden air

TABLE I

SUMMARY OF EXAMPLE REENTRAINMENT
CALCULATIONS FOR THE GPC

Surface	Case (1) (Smooth)	Case (2) (Rough)
u_{*t}, cm/s	28	28
u_*, cm/s	31.8	38.5
Δt, s	2.25	4.50
q_v, g/(cm^{2}s)	2.77 x10^{-8}	5.61 x 10^{-5}
M, g	0.03	119
$u_d (=u_f)$, cm/s	5.74	5.74
Deposition rate, g/s	--	1.15
Depletion time, s	--	103

reaching the environment. The variation of flow in the branches of interest can be examined to find potential problem areas if entrainment does take place. This limits the entrainment studies to only the potentially important areas. Figure 6 summarizes this procedure for the GPC of the NFS facility using computerized plots. These plots show the relationship between the period when the steady-state velocity is exceeded, when flows are entering or leaving the cell boundaries, and when flows are entering or leaving the ventilation system boundaries. The area under the flow curve represents the amount of air moved. The exact value of this integral can be found from the integrated flows tabulated in the TVENT output such as shown in Fig. A-2. The only flows out of the GPC during or after the period when the floor velocity exceeds its threshold value are to the PMC through branch 7 and out through branch 8, the 0.5-m exhaust duct. The latter flow passes through the filter plenums before being exhausted to the environment and thus may not represent a threat. A portion of the air flowing back into the PMC may contain airborne particulate if reentrainment occurs. However, the direction of the flow in branch 4, the PMC outside air supply connection, indicates that none of the contaminated air returning to the PMC from the GPC reaches the environment. Therefore, although reentrainment does occur in the GPC, the suspended material will not likely reach an atmospheric boundary.

VII. SUMMARY

This report has presented an analytical procedure that may be used to calculate particulate release from nuclear fuel fabrication or reprocessing facilities subject to tornado transient conditions. As an example, this procedure was applied to part of an existing fuel reprocessing plant. The plant ventilation system was modeled using a computer code that predicts flows and pressures throughout the system. A second computer code calculated velocities in a particular process cell. Then a new approach was used to estimate a quantity of suspended material for two surface conditions. For the case of a rough surface (equivalent to the roughness of medium-sized sand particles) we found that about 119 g of particulate could become suspended. However, consideration of the flow rate magnitudes and directions revealed that even for this case a release would be unlikely. While this finding is significant, the purpose of the report was to illustrate the analysis procedure for a tornado accident
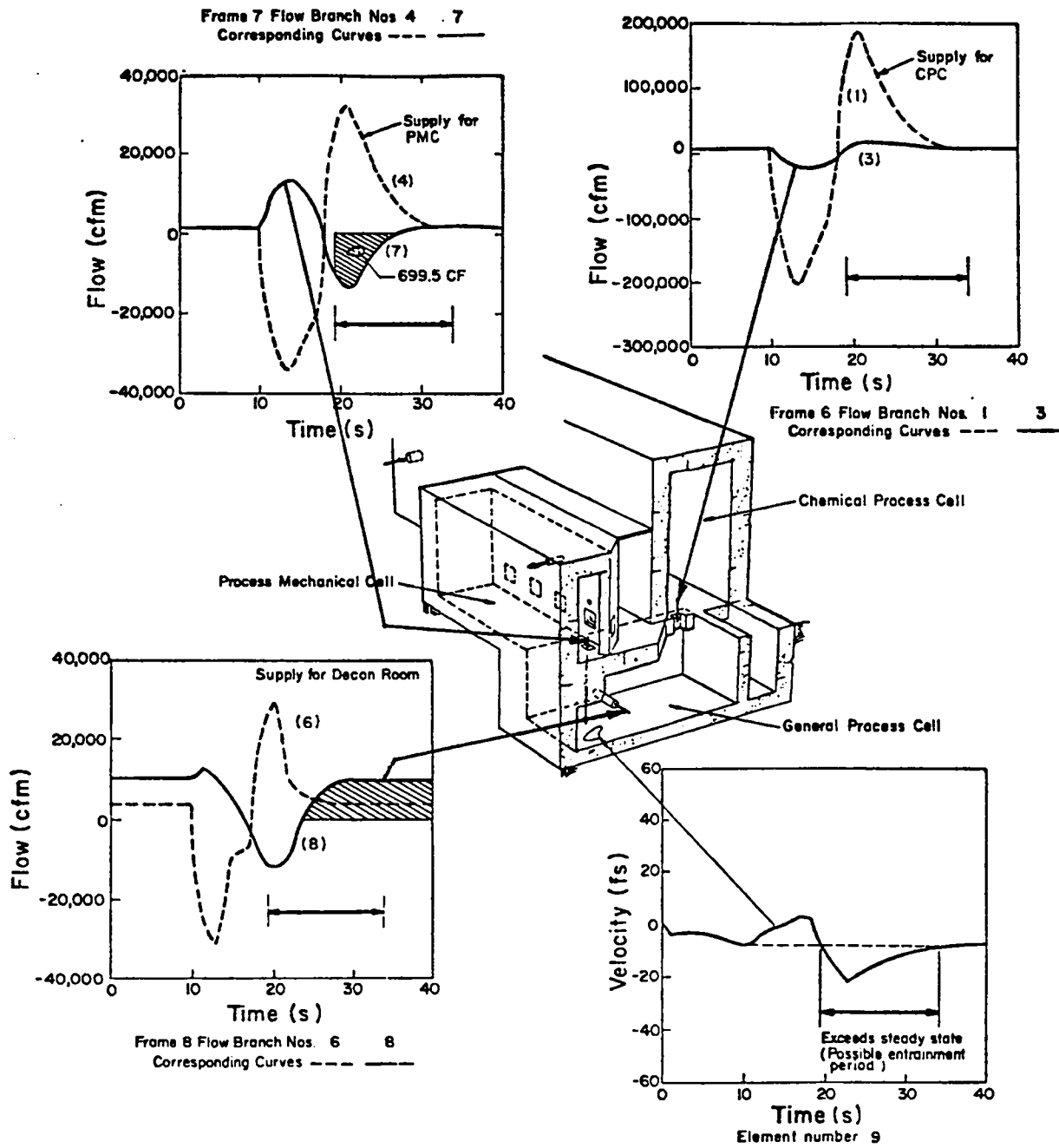
Fig. 6.
Composite of computerized plots for defining entrainment problems.

NOTE: 1 cfm = 4.719 x 10^{-4} m^3/s
       1 f/s = 0.3048 m/s

17

condition. We believe that this procedure affords much greater potential for accuracy than the resuspension factor approach or one that simply assumes all of the material is reentrained. Therefore, we feel that further study is warranted and should be pursued.

APPENDIX A

TVENT DATA

```
                    TVENT                LASL
               L I S T   O F   I N P U T   D A T A
         10        20        30        40        50        60        70        80
   12345678901234567890123456789012345678901234567890123456789012345678901234567890
1**
2*NFS HEAD-END VENT, SYSTEM, TORNADO AT ALL BOUNDARY NODES EXCEPT EXHAUST
3**
4**  RUN CONTROL I
5*        .1   40.      50
6**  PRINT/PLOT CONTROL
7*              3
8**  FRAME DESCRIPTIONS
9*    2    1    3
10*   2    4    7
11*   2    6    8
12**  RUN CONTROL II
13*  5000                      P
14**  BOUNDARY CONTROL
15*    1    4
16**  GEOMETRY AND COMPONENT CONTROL
17*   21   20    2    7    1
18**  BRANCHES
19*    1    1    20583.                    V
20*    2    2    30583.                    F
21*    3    3    00583.      9.575         V
22*    4    4    51727.                    V
23*    5    5    61727.                    F
24*    6    7    93900.                    V
25*    7    6    81727.      10.15         V
26*    8    8  1010310.       5.0          V
27*    9   19   103900.                    V
28*   10   20   111021A.                   F
29*   11   11  1214210.                    F
30*   12   12  1314210.                    F
31*   13   13  1414210.                    F
32*   14   14  1614210.                    V
33*   15   16   157105.                    B                         1
34*   16   16   157105.                    B                         1
35*   17   15  1714210.                    V
36*   18    9   181900.                    V
37*   19    9  1920A0.                     V
38*   20   18   191900.                    V
39*   21   10  2014210.                    V
40**  BOUNDARY DATA
41*    1            1
42*    4            1
43*    7            1
44*   17
45**  TORNADO TRANSIENT
46*    1    5
47*0.0        0.0        10.0        0.0        13.25      -72.0
48*17.25     -72.0      20.50       0.0
49**  ROOM DATA
50*   1510.       10.         30.
51*    910.       10.         75.20
52*    210.       10.        250.
53*    310.       10.        879.8
54*    510.       10.        150.
55*    610.       10.        155.
56*    810.       10.         47.8
57**  BLOWER CURVE
58*    1    6
59**-2000.      35.0        0.         23.0       3500.      22.6
60*7105.       20.A0      10000.       12.0      12000.       0.
61**  PRESSURES
62*    0.          -.05          -.9          0.0          -.10
63*   -1.80         0.          -1.81        -0.15         -6.5
64*   -7.7         -9.7         -18.2        -19.5          0.4
65*  -19.6          0.0          -5.5         -5.8         -7.2
```

Fig. A-1.
Echo of input to TVENT.

BRANCH	TIME	FLOW	INT. FLOW	AVE. VEL.
3	23.90000	14986.84	788.84	31.22
7	23.90000	-5381.17	528.89	-9.83
8	23.90000	2853.08	1653.73	15.68
3	24.00000	14913.54	812.95	31.07
7	24.00000	-5026.73	520.28	-9.32
8	24.00000	2455.78	1657.49	18.76
3	24.10000	14824.82	837.74	30.88
7	24.10000	-4757.68	512.13	-8.82
8	24.10000	2835.92	1661.90	21.66
3	24.20000	14723.16	862.36	30.67
7	24.20000	-4494.16	504.42	-8.33
8	24.20000	3195.41	1666.92	24.41
3	24.30000	14610.59	886.80	30.44
7	24.30000	-4236.26	497.14	-7.85
8	24.30000	3536.89	1672.53	27.01
3	24.40000	14488.87	911.05	30.18
7	24.40000	-3984.85	490.29	-7.39
8	24.40000	3859.58	1678.78	29.49
3	24.50000	14359.34	935.89	29.91
7	24.50000	-3737.69	483.85	-6.93
8	24.50000	4166.90	1685.39	31.83
3	24.60000	14223.28	958.91	29.63
7	24.60000	-3497.18	477.83	-6.48
8	24.60000	4459.30	1692.57	34.07
3	24.70000	14081.76	982.50	29.33
7	24.70000	-3262.56	472.19	-6.05
8	24.70000	4737.76	1700.24	36.19
3	24.80000	13935.73	1005.85	29.03
7	24.80000	-3033.86	466.95	-5.62
8	24.80000	5003.16	1708.36	38.22
3	24.90000	13786.85	1028.95	28.72
7	24.90000	-2811.09	462.07	-5.21
8	24.90000	5256.28	1716.91	40.16
3	25.00000	13633.41	1051.88	28.40
7	25.00000	-2594.30	457.57	-4.81
8	25.00000	5497.70	1725.87	42.00
3	25.10000	13478.59	1074.39	28.08
7	25.10000	-2383.43	453.42	-4.42
8	25.10000	5728.30	1735.22	43.76
3	25.20000	13322.19	1096.73	27.75
7	25.20000	-2178.52	449.62	-4.04
8	25.20000	5948.55	1744.95	45.44
3	25.30000	13164.73	1118.80	27.42
7	25.30000	-1979.62	446.16	-3.67
8	25.30000	6158.83	1755.04	47.05
3	25.40000	13006.79	1140.61	27.10
7	25.40000	-1786.64	443.02	-3.31
8	25.40000	6359.88	1765.47	48.59
3	25.50000	12848.85	1162.15	26.77
7	25.50000	-1599.63	440.19	-2.97
8	25.50000	6552.01	1776.23	50.05
3	25.60000	12691.28	1183.44	26.44
7	25.60000	-1418.63	437.68	-2.63
8	25.60000	6735.54	1787.31	51.46
3	25.70000	12534.59	1204.46	26.11
7	25.70000	-1243.54	435.46	-2.31
8	25.70000	6911.06	1798.68	52.80
3	25.80000	12379.13	1225.22	25.79
7	25.80000	-1074.40	433.53	-1.99
8	25.80000	7078.84	1810.34	54.08

Fig. A-2.
Velocity and integrated flow printout.
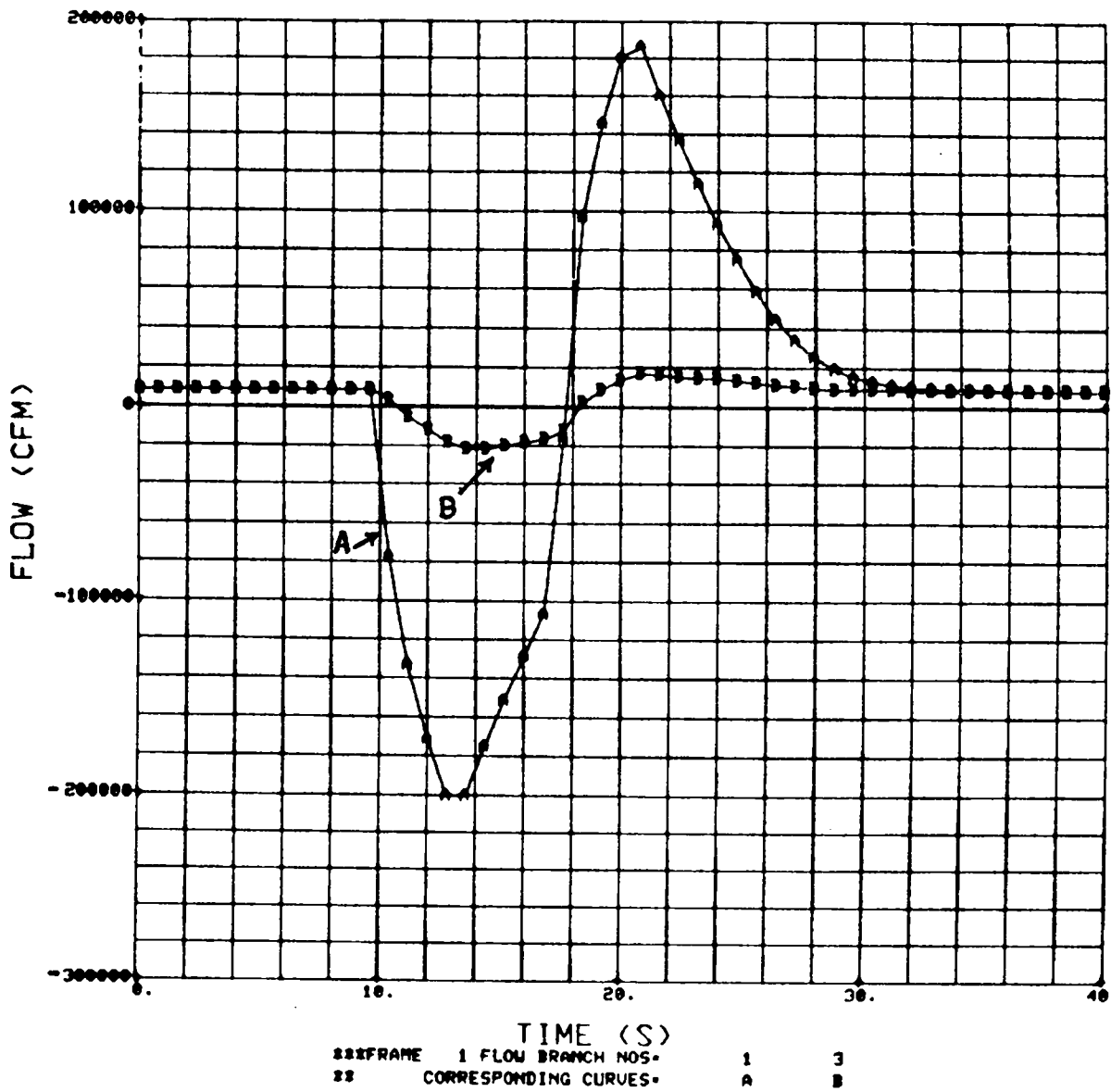
Fig. A-3.
TVENT plot showing induced flows.
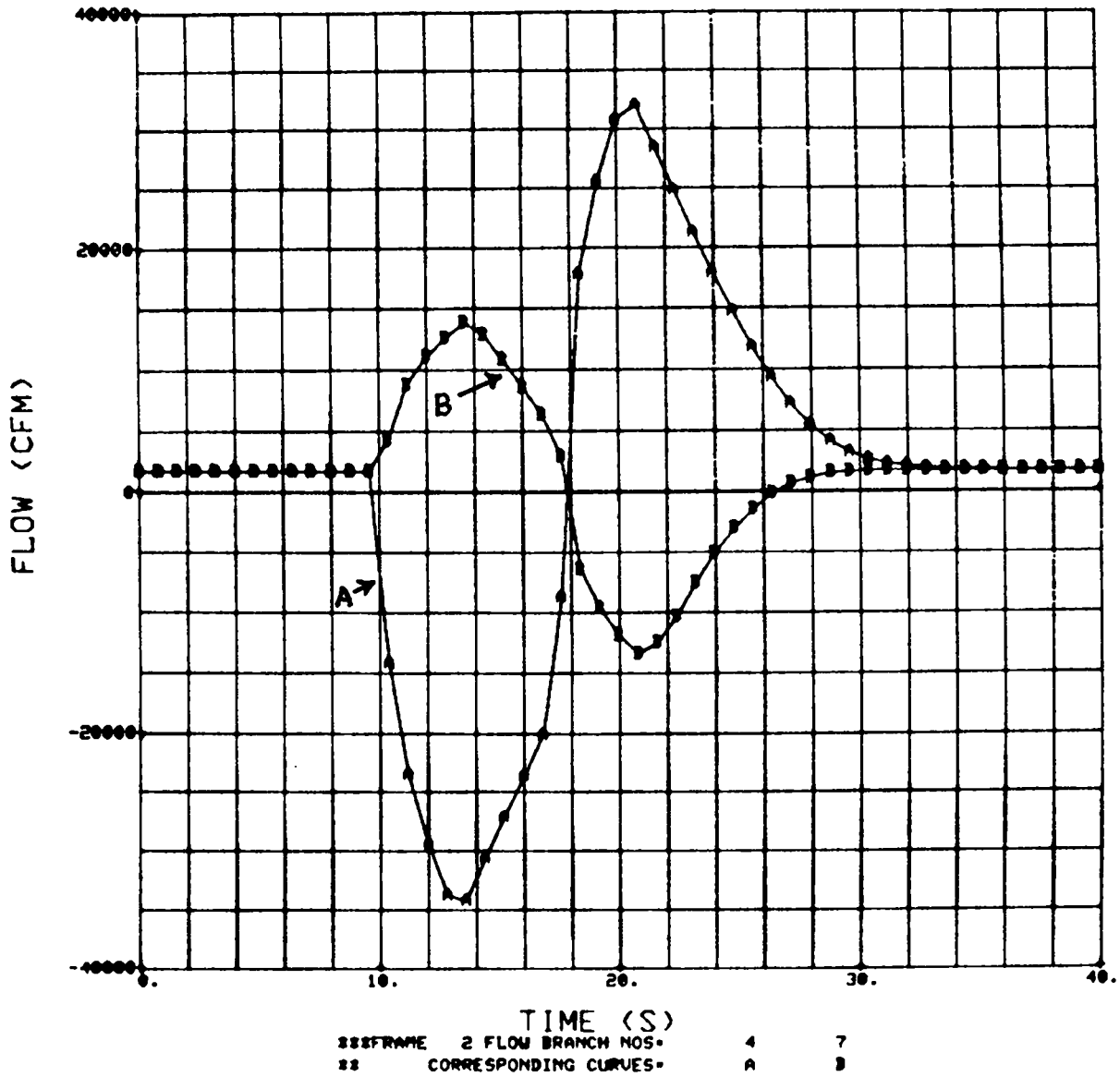
NOTE: 1 cfm = 4.719 x 10^{-4} m^3/s

Fig. A-4.
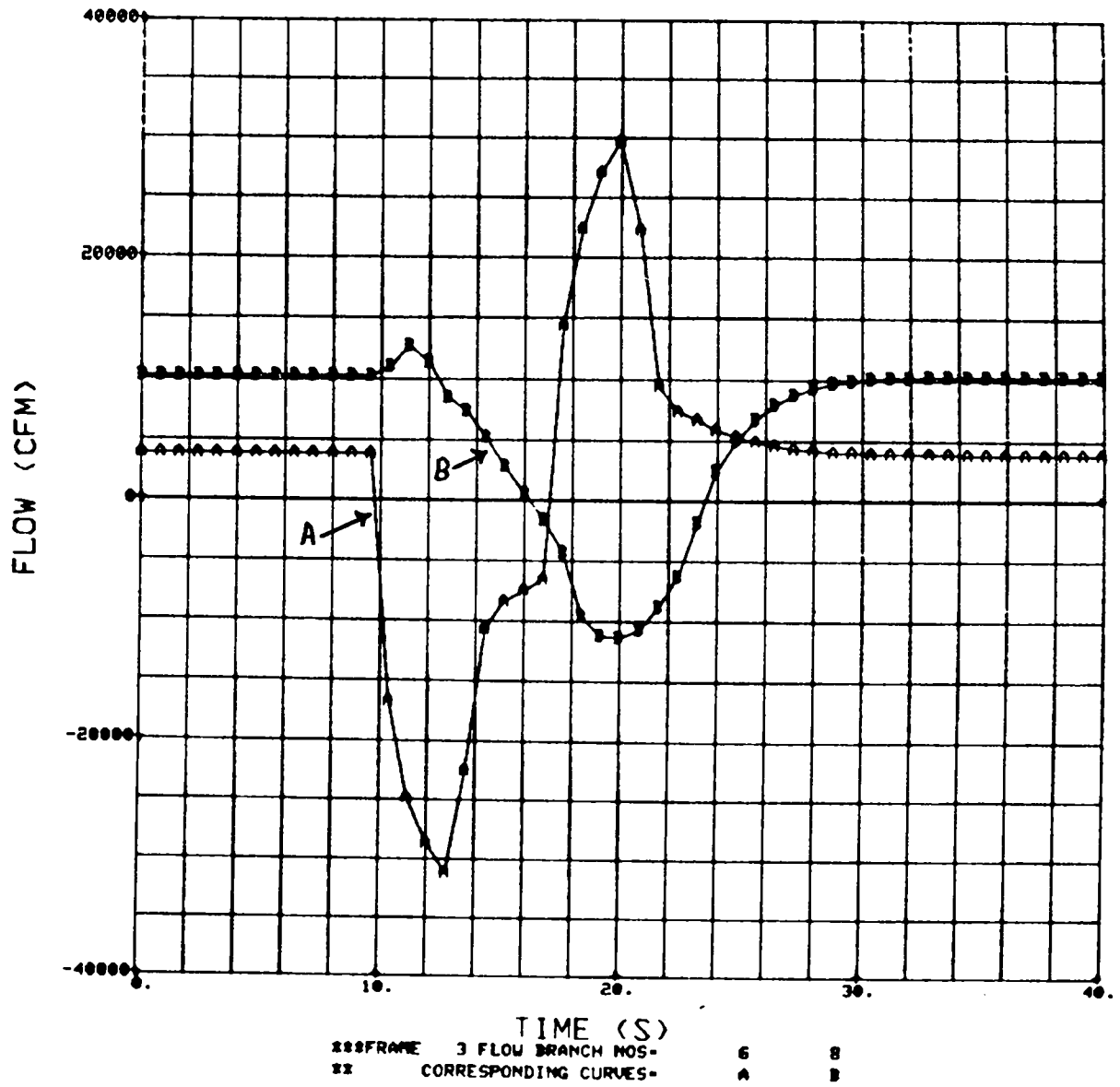TVENT plot showing induced flows.

NOTE: 1 cfm = 4.719 x 10^{-4} m³/s

Fig. A-5.
TVENT plot showing induced flows.

NOTE: 1 cfm = 4.719 x 10^{-4} m³/s

SOLA-ICE DATA

NFS HEAD-END VENT. SYSTEM, TORNADO AT ALL BOUNDARY NODES EXCEPT EXHAUST

```
      IBAR=  1.20000E+01
      JBAR=  1.50000E+01
      DELX=  1.67000E+00
      DELY=  3.00000E+00
      DELT=  1.00000E-03
     TWFIN=  4.00000E+01
     CWPRT=  1.00000E+03
     CWPLT=  1.00000E+03
       CYL=  0.
        GX=  0.
        GY=  0.
        UI=  0.
        VI=  0.
     VELMX=  8.00000E+01
        WL=      1
        WB=      1
        WR=      1
        WT=      1
        NU=  1.49000E-01
      EPSI=  1.00000E-03
        PR=  7.00000E-01
       OMG=  5.00000E-01
     ALPHA=  1.00000E+00
      GAM1=  4.00000E-01
       ASQ=  0.
       ROI=  2.33000E-03
     T AMB=  5.30000E+02
   DRIVE T=  5.30000E+02
    MOL WT=  2.90000E+01
      RGAS=  4.96900E+04
     DTVNT=  .10000E+00
    DTSOLI=  .10000E-02
      NTSP=    401
      NVTF=      5
   MULT. V(1) BY        1.00
   MULT. V(2) BY        1.00
   MULT. V(3) BY        1.00
   MULT. V(4) BY        1.00
   MULT. V(5) BY       -1.00
   MULT. V(6) BY
  2  NELB=       4
  3  NELB=       0
  4  NELB=       0
  5  NELB=       0
  6  NELB=       0
  7  NELB=       0
  8  NELB=       0
  9  NELB=       0
 10  NELB=       0
 11  NELB=       0
 12  NELB=       0
 13  NELB=       0
 14  NELB=       0
 15  NELB=       0
 16  NELB=       2
  2  NEBB=       0
  3  NEBB=       0
  4  NEBB=       5
```

```
  5  NEBB=       0
  6  NEBB=       0
  7  NEBB=       0
  8  NEBB=       0
  9  NEBB=       0
 10  NEBB=       0
 11  NEBB=       0
 12  NEBB=       0
 13  NEBB=       0
  2  NERB=       0
  3  NERB=       0
  4  NERB=       0
  5  NERB=       0
  6  NERB=       0
  7  NERB=       0
  8  NERB=       0
  9  NERB=       0
 10  NERB=       0
 11  NERB=       0
 12  NERB=       0
 13  NERB=       0
 14  NERB=       0
 15  NERB=       0
 16  NERB=       0
  2  NETB=       0
  3  NETB=       0
  4  NETB=       0
  5  NETB=       0
  6  NETB=       0
  7  NETB=       0
  8  NETB=       0
  9  NETB=       0
 10  NETB=       0
 11  NETB=       0
 12  NETB=       0
 13  NETB=       0
  OUTPUT OPTION=       3
  BEGIN. TSTEP=       1
  BEGIN. TIME=      0.
  VMAX =      0.
  VMIN =      0.
  NEL1=       4
  NEL2=       9
  NEL3=      14
```
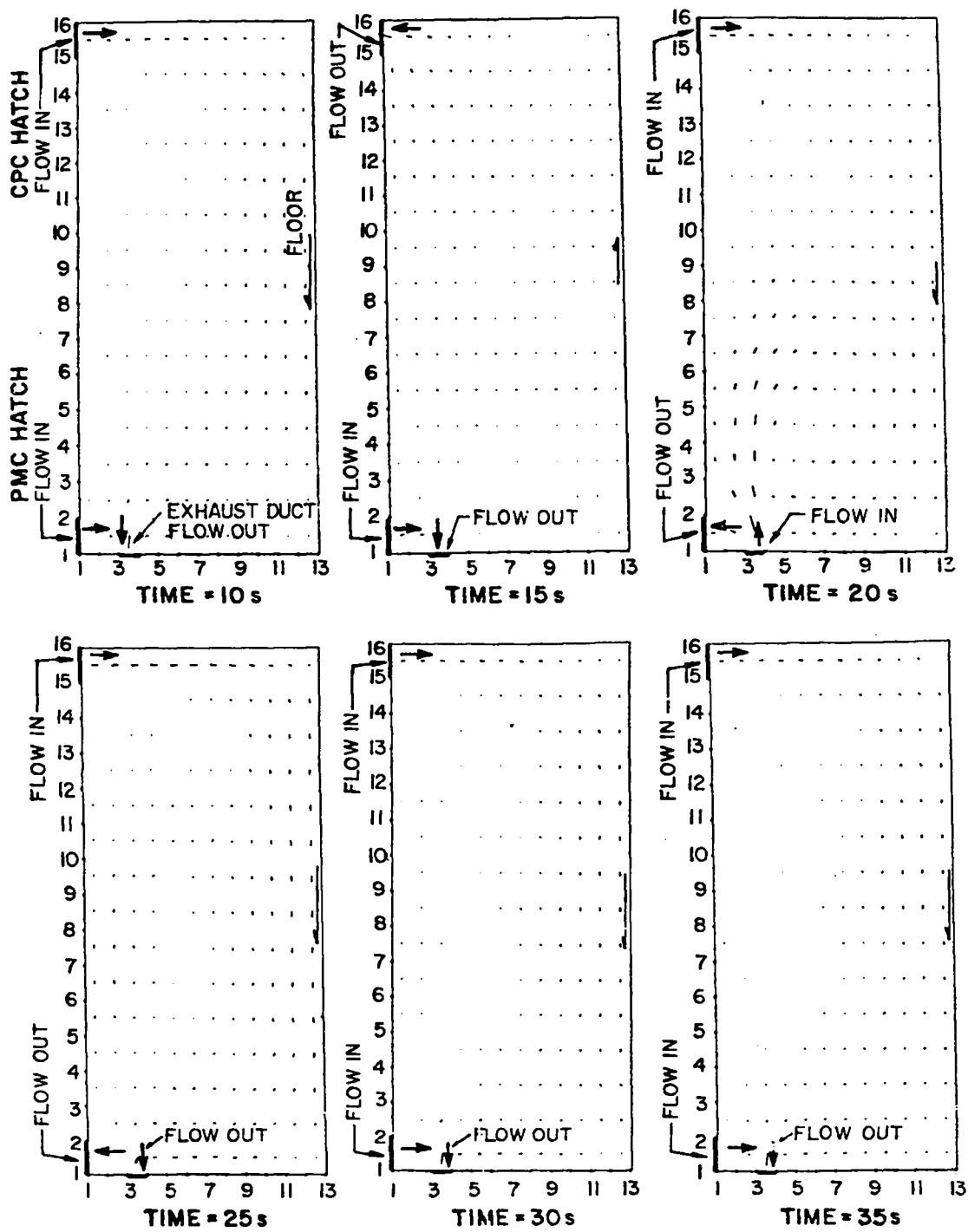
Fig. B-1.
SOLA-ICE input data.

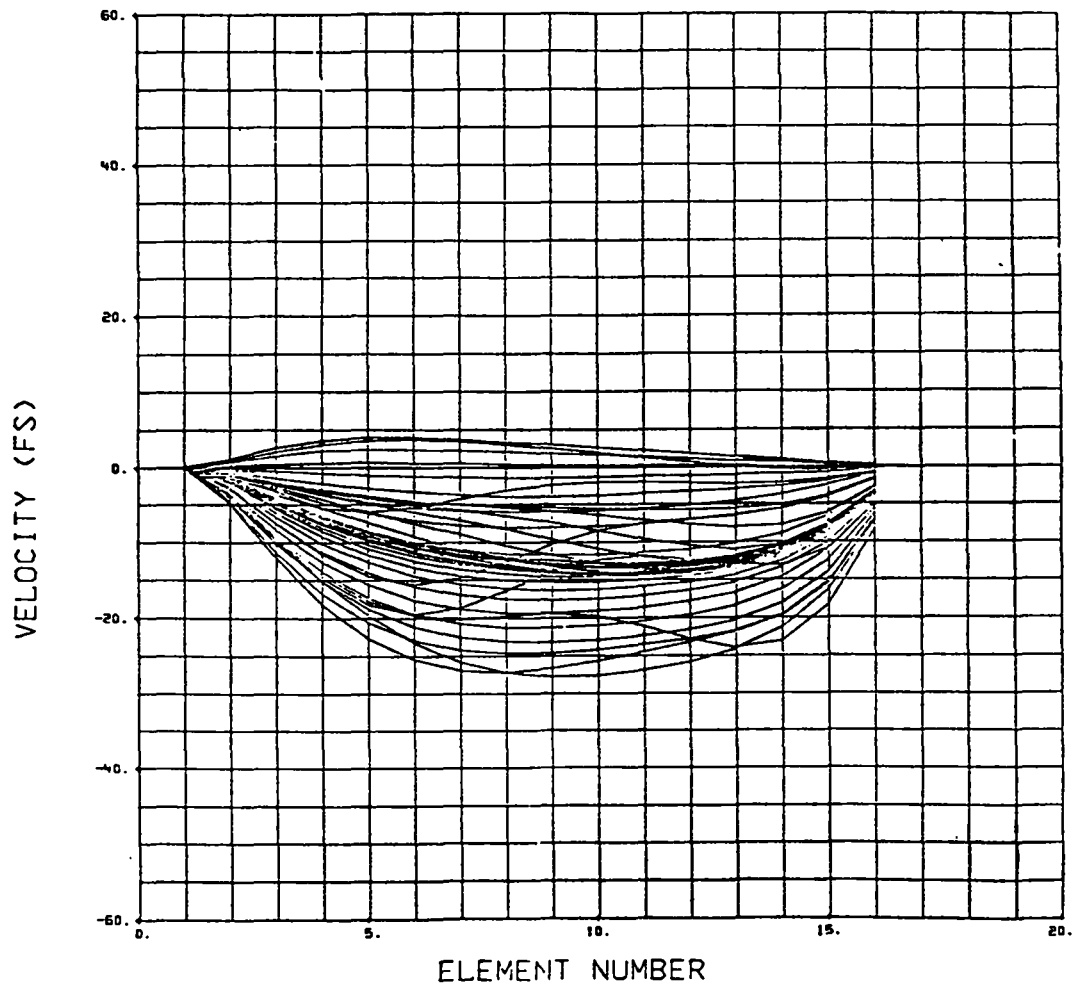Fig. B-2.
Composite of SOLA-ICE velocity vector plots.

Fig. B-3.
SOLA-ICE plots for envelope of floor velocity curves.

NOTE: Each curve represents the spatial distribution
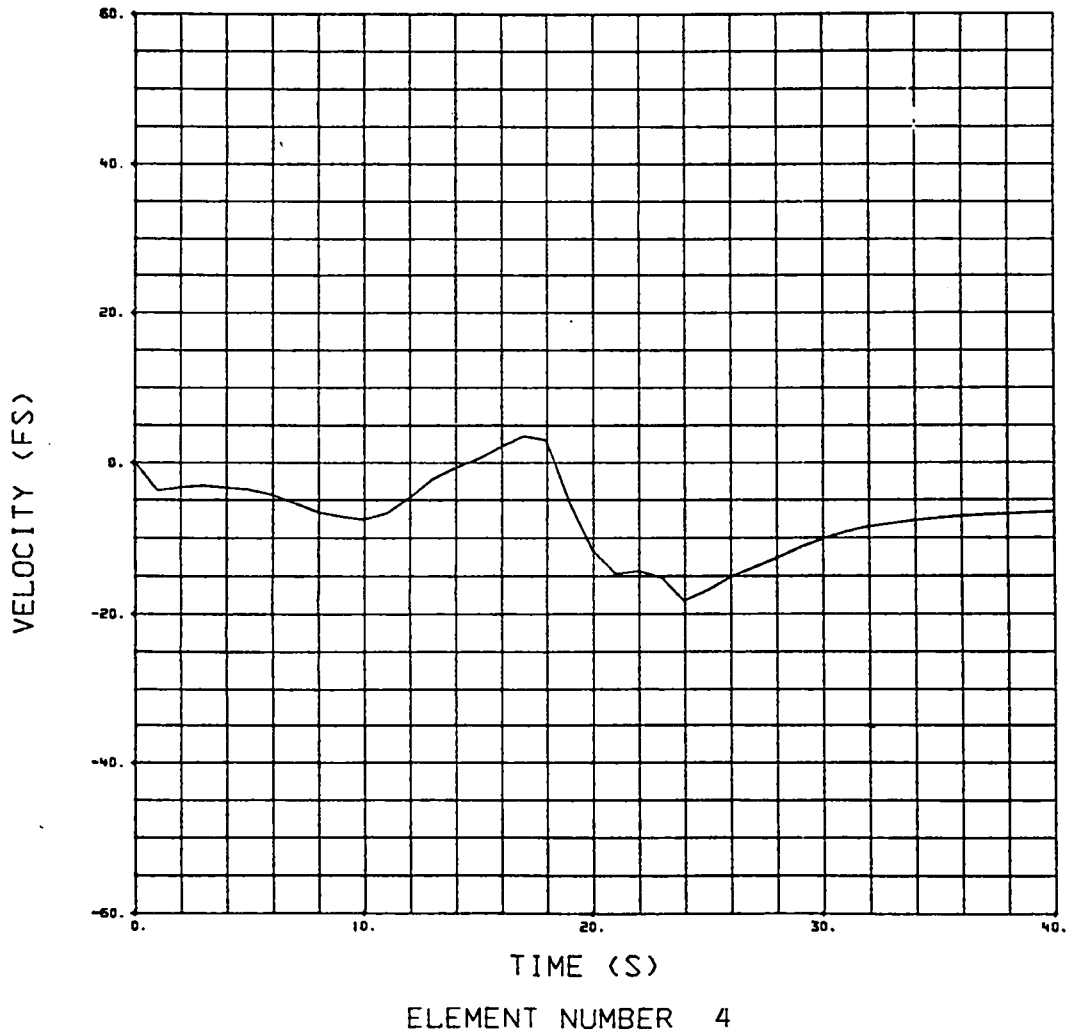of velocity at a given time. 1 ft/s = 0.3048 m/s.

VELOCITY (FS)

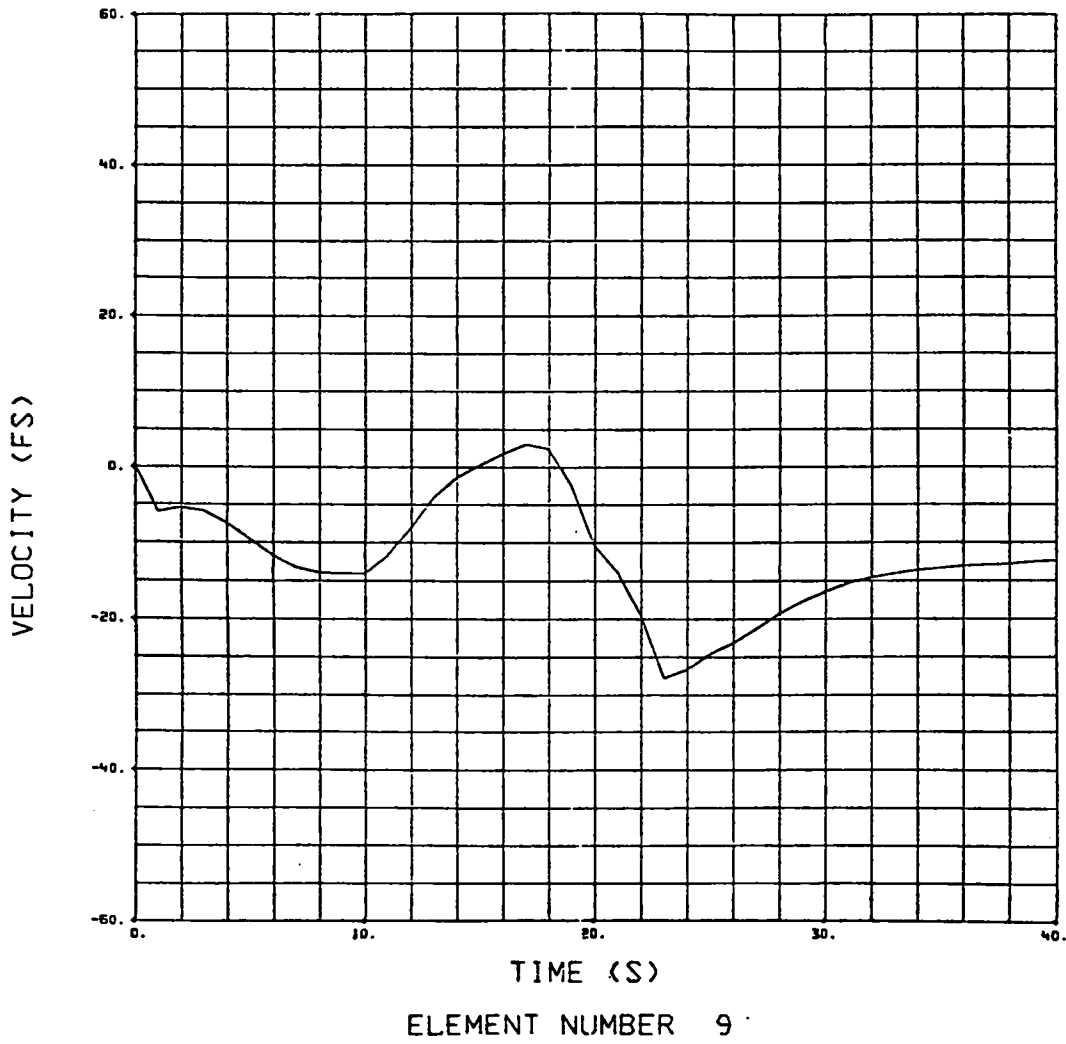TIME (S)

ELEMENT NUMBER   4

Fig. B-4.
SOLA-ICE plot showing velocity history at element 4.

NOTE: 1 ft/s = 0.3048 m/s.

27

Fig. B-5.
SOLA-ICE plot showing velocity history at element 9.
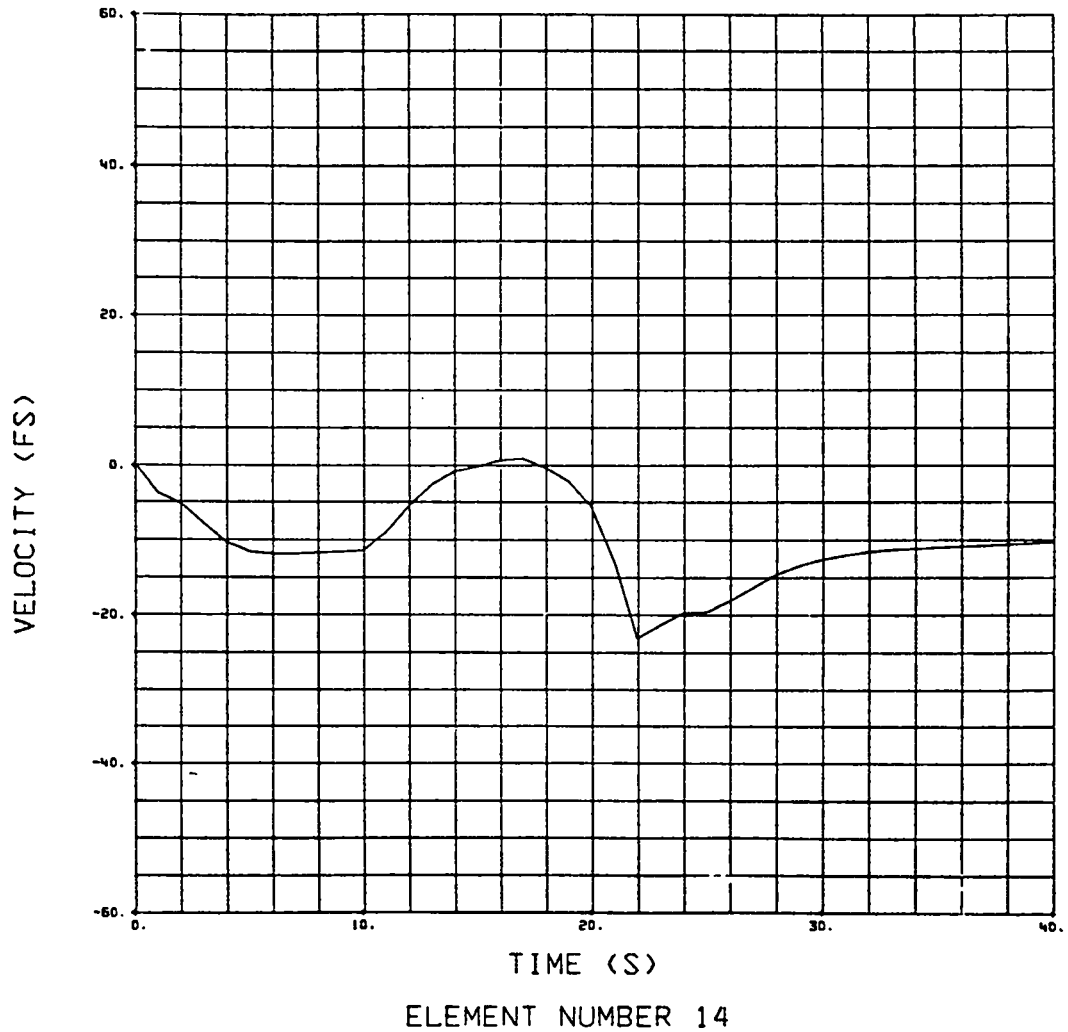
NOTE: 1 ft/s = 0.3048 m/s.

Fig. B-6.
SOLA-ICE plot showing velocity history at element 14.

NOTE: 1 ft/s = 0.3048 m/s.

```
ITER=    1         TIME= 2.400000E+01         CYCLE= 24000
VEL. TF NO. =  1      VELOCITY =  1.92E+02
VEL. TF NO. =  2      VELOCITY =  3.11E+01
VEL. TF NO. =  3      VELOCITY =  5.32E+01
VEL. TF NO. =  4      VELOCITY = -9.32E+00
VEL. TF NO. =  5      VELOCITY =  1.88E+01
 I    J      VEL(X)           VEL(Y)           VEL(T)
13    2    -2.24397E+00     -4.18680E+00      4.75023E+00
13    3    -1.87956E+00     -1.19078E+01      1.20552E+01
13    4    -1.41470E+00     -1.81261E+01      1.81812E+01
13    5    -9.45888E-01     -2.26303E+01      2.26501E+01
13    6    -5.25547E-01     -2.54931E+01      2.54985E+01
13    7    -1.79975E-01     -2.69352E+01      2.69358E+01
13    8     8.62212E-02     -2.72426E+01      2.72427E+01
13    9     2.68491E-01     -2.67291E+01      2.67304E+01
13   10     3.66492E-01     -2.57116E+01      2.57142E+01
13   11     3.90347E-01     -2.44798E+01      2.44829E+01
13   12     3.85954E-01     -2.32225E+01      2.32257E+01
13   13     4.61317E-01     -2.18504E+01      2.18553E+01
13   14     8.18730E-01     -1.97169E+01      1.97339E+01
13   15     1.77349E+00     -1.52529E+01      1.53557E+01
13   16     3.49925E+00     -6.08611E+00      7.02036E+00


ITER=    1         TIME= 2.500000E+01         CYCLE= 25000
VEL. TF NO. =  1      VELOCITY =  1.48E+02
VEL. TF NO. =  2      VELOCITY =  2.84E+01
VEL. TF NO. =  3      VELOCITY =  4.80E+01
VEL. TF NO. =  4      VELOCITY = -4.81E+00
VEL. TF NO. =  5      VELOCITY =  4.20E+01
 I    J      VEL(X)           VEL(Y)           VEL(T)
13    2    -2.19911E+00     -4.01067E+00      4.57401E+00
13    3    -1.76187E+00     -1.12516E+01      1.13887E+01
13    4    -1.25583E+00     -1.67926E+01      1.68395E+01
13    5    -8.06020E-01     -2.05907E+01      2.06965E+01
13    6    -4.59982E-01     -2.29294E+01      2.29348E+01
13    7    -2.13955E-01     -2.41773E+01      2.41783E+01
13    8    -4.11689E-02     -2.46501E+01      2.46502E+01
13    9     7.92075E-02     -2.45835E+01      2.45836E+01
13   10     1.54255E-01     -2.41649E+01      2.41653E+01
13   11     1.97261E-01     -2.35393E+01      2.35401E+01
13   12     2.44274E-01     -2.27598E+01      2.27611E+01
13   13     3.81997E-01     -2.16575E+01      2.16609E+01
13   14     7.87549E-01     -1.95914E+01      1.96072E+01
13   15     1.74408E+00     -1.51007E+01      1.52011E+01
13   16     3.39871E+00     -6.00192E+00      6.89741E+00
```

Fig. B-7.
Example of the numerical velocity data from SOLA-ICE.

NOTE: I and J refer to the y and x axes, respectively, in Fig. 4.

EQUATIONS AND PROCEDURE FOR REENTRAINMENT CALCULATION

The equations and procedure presented in this appendix were discussed in more detail in Ref. 7.

The first question we must answer is: When do the particles begin to move? Before particle motion can occur, a threshold air speed must be equalled or exceeded so that the aerodynamic forces will be sufficient to overcome restraining forces. To relate threshold air speed to surface effects, we introduce the friction speed

$$u_* = \sqrt{\tau/\rho} , \tag{C-1}$$

where τ = mean shear stress at the surface and
ρ = fluid density.

Experimental measurements of <u>threshold</u> friction speed u_{*t} are available for a wide range of material sizes and densities.[10]

These measurements were plotted in Fig. 5 (from Ref. 10) and are fitted to the following semi-empirical equation.

$$A = (0.108 + 0.0323/B - 0.00173/B^2) \tag{C-2}$$

$$\times (1 + 0.055/\rho_p g \, D_p^2)^{1/2} ,$$

where $A = u_{*t}/[(\rho_p - \rho) \, gD_p/\rho]^{1/2}$,

ρ_p = particle density,
g = gravitational acceleration,
D_p = average particle diameter,
$B = u_{*t}D_p/\upsilon$, and
$\upsilon = \mu/\rho$ = fluid kinematic viscosity.

Equation (C-2) holds for $0.22 \le B \le 10$ and accounts for particle weight, interparticle forces, and aerodynamic forces.

We may relate u_* to the corresponding velocity at the turbulent boundary layer edge using one of the following two equations. For a smooth surface with a laminar sublayer,[12]

$$u(y)/u_* = (1/0.41) \ln (yu_*/\upsilon) + 5.0 \ . \qquad (C-3)$$

For a rough surface with no laminar sublayer,[13]

$$u(y)/u_* = (1/k) \ln (y/y_0) \ , \qquad (C-4)$$

where y = distance from surface,

    k = 0.4 = Von Karman constant,

    y_0 = R/30 = roughness length, and

    R = average surface roughness height.

The next question is: What determines whether particles go into suspension? That is, of all the particles, how do we divide those that could become airborne from those that remain close to the surface? Iversen et al.,[11] have shown that for particles smaller than 52 m, suspension occurs as soon as the threshold speed is reached. The criterion assumed here was that suspension will occur for those particles for which $u_f/u_* = 1$ and $u_* > u_{*t}$, where u_f is the particle fall or terminal speed. The friction speed u_* is of the same order of magnitude as the vertical component of turbulence in a boundary layer. Values of $D_p < 50 \ \mu m$ for suspension are in agreement with measurements using soils.[8] In the present exercise, since we assumed $D_p < 50 \ \mu m$, all of the particles are therefore subject to suspension.

How much material becomes suspended? Travis[8] has suggested the following expression for q_v, the mass of particles per unit area per unit time that go into suspension:

$$q_v = q_h (c_v/u_{*t}c_h) (u_*/u_{*t})^{P/3-1} \ , \qquad (C-5)$$

where P = mass percentage of suspendable particles and

    c_v, c_h = empirical constants (2×10^{-10} and 10^{-6}, respectively).

In Eq. (C5) q_h is the mass of material moving horizontally through a vertical plane perpendicular to the surface per unit width per unit time and may be determined from[9]

32

$$q_h = 2.61(\rho/g)(u_* + u_{*t})^2(u_* - u_{*t}) \ . \tag{C-6}$$

The last question is: Does the material stay suspended or does it redeposit? A rough estimate of the quantity of particulate that will deposit may be obtained from[14]

$$u_d = \frac{\text{mass deposition/cm}^2\text{s}}{(\text{mass/cm}^3) \text{ concentration above surface}} \ , \tag{C-7}$$

provided we assume $u_d = u_f$. The latter assumption is equivalent to neglecting any deposition mechanism other than gravitational settling. An estimate of u_f may be obtained from[15]

$$u_f = D_p^2 g \ (\rho_p - \rho)/18\mu \ . \tag{C8}$$

APPENDIX D

MODIFICATIONS TO SOLA-ICE

The input/output formats of SOLA-ICE[4] were changed to make the code more useful as a tool in solving for velocity distributions in a cell or room. Some of the important changes involved input of velocity from TVENT on punched cards, the application of these velocity functions at any desired boundary element and the inclusion of output options to limit the amount of output data. The input card deck is organized into five categories as follows.

● problem definition,

● fluid properties,

● velocity function deck,

● boundary conditions, and

● output options.

The card formats are given below:

1. Title (8A10)

2. Number of entries to be read set to 30 (15)

3. $\left.\begin{array}{l}\\\\\end{array}\right\}$

4. Problem definition (6E10.2)

5.

       IBAR, JBAR, DELX, DELY, DELT, TWFIN, CWPRT, CWPLT, CYL, GX, GY, UI,

       VI, VELMX, WL, WB, WR, and WT

6. Fluid properties (6E10.2) $\left.\begin{array}{l}\\\\\end{array}\right\}$

7.

   These cards may be left blank if the fluid is air and the units are English.

8. Control for interfacing TVENT to SOLA-ICE (2E10.2)

       TVENT delta time step, SOLA-ICE delta time step.

9. Control for reading TVENT velocity deck (2I5)

       Number of time steps, number of time functions.

10.

    •

    •

  .deck containing "m" cards $\left.\begin{array}{l}\\\\\\\\\\\\\end{array}\right\}$

    •

    •

10 + n

10 + (n + 1)   Load factor for time functions (6E10.2)

10 + (n + 2)   Time function or functions in left boundary elements (1X,79I1)

10 + (n + 3)   Time function or functions in bottom boundary elements (1X,79I1)

10 + (n + 4)   Time function or functions in right boundary elements (1X,79I1)

10 + (n + 5)   Time function or functions in top boundary elements (1X,79I1)

10 + (n + 6)   Output options (2I5,3E10.2, 3I5)

            Printed velocities,

               1 -- average velocities in elements adjacent to left boundary

               2 -- average velocities in elements adjacent to bottom boundary

               3 -- average velocities in elements adjacent to right boundary

4 -- average velocities in elements adjacent to top boundary

5 -- average velocities in all elements starting card number in velocity function deck, beginning time, maximum vertical velocity on envelope plot, and minimum vertical velocity on envelope plot, element number for velocity vs time plot, element number for velocity vs time plot, and element number for velocity vs time plot.

REFERENCES

1. W. S. Gregory, R. W. Andrae, K. H. Duerre, and R. C. Dove, "Ventilation Systems Analysis under Tornado Conditions," Los Alamos Scientific Laboratory report LA-6999-PR (October 1977).

2. G. A. Bennett, W. S. Gregory, and P. R. Smith, "Ventilation System Analysis During Tornado Conditions," Los Alamos Scientific Laboratory report LA-6120-PR (November 1975).

3. R. W. Andrae, K. H. Duerre, and W. S. Gregory, "TVENT--A Computer Program for Analysis of Tornado Induced Transients in Ventilation Systems," Los Alamos Scientific Laboratory report LA-7397-M (July 1978).

4. L. D. Cloutman, C. W. Hirt, and N. C. Romero, "SOLA-ICE - A Numerical Solution Algorithm for Transient Compressible Fluid Flows," Los Alamos Scientific Laboratory report LA-6236 (July 1976).

5. J. E. Kahn, Oak Ridge National Laboratory, personal communication to R. W. Andrae, Los Alamos Scientific Laboratory, September 1977.

6. J. W. Healy, "Surface Contamination: Decision Levels," Los Alamos Scientific Laboratory report LA-4558-MS (September 1971).

7. R. A. Martin, "Reentrainment of Particulate Contaminants in Ventilation Systems Subject to Flows Induced by Tornado Transients," Los Alamos Scientific Laboratory report to be published.

8. J. R. Travis, "A Model for Predicting the Redistribution of Particulate Contaminants from Soil Surfaces," Los Alamos Scientific Laboratory report LA-6035-MS (August 1975).

9. J. D. Iversen, R. Greeley, B. R. White, and J. B. Pollack, "The Effect of Vertical Distortion in the Modeling of Sedimentation Phenomena: Martian Crater Wake Streaks," J. Geophys. Res. 81, No. 26, 4846-4856 (1976).

10. J. D. Iversen, J. B. Pollack, R. Greeley, and B. R. White, "Saltation Threshold on Mars: The Effect of Interparticle Force, Surface Roughness, and Low Atmospheric Density," ICARUS <u>29</u>, 381-393 (1976).

11. J. D. Iversen, R. Greeley, and J. B. Pollack, "Windblown Dust on Earth, Mars and Venus," J. Atm. Sci. <u>33</u>, No. 12, 2425-2429 (1976).

12. F. M. White, <u>Viscous Fluid Flow</u> (McGraw-Hill Book Company, Inc., New York, 1974).

13. H. Schlichting, <u>Boundary Layer Theory</u> (McGraw-Hill Book Company, Inc., 4th Ed., New York, 1960).

14. C. N. Davies, "The Deposition of Particles from Moving Air," in <u>Surface Contamination</u>, B. R. Fish, Ed. (Pergamon Press, New York, 1967).

15. R. S. Brodkey, <u>The Phenomena of Fluid Motions</u> (Addison-Wesley, Reading, Massachusetts, 1967).